



SINGAPORE UNIVERSITY OF
TECHNOLOGY AND DESIGN

40.018 Heuristics and Systems Theory

Project 2

CS02

Name	Student ID	Contribution
Benedict Nai Rong Hui	1008173	Report Sections 3, 4 and 5
Mika Ling	1007901	Report Sections 1, 2 and 6
Muk Chen Eu Zachary	1007848	MATLAB Code, Derivation of Mathematical Formulas

1 Introduction

Diabetes and glucose management have always been significant points of interest in the field of medicine. Type 2 diabetes is especially prominent, given that it represents 95% of patients with diabetes (World Health Organization, 2024).

Consequently, many experts have developed ways in their fields to improve glucose control methods. As diabetes is a multifaceted condition with different variables involved, biomedical engineers have derived various models to simulate systemic interactions between insulin and glucose. Given the prevalence of diabetes and the existence of such models, this project aims to analyse, define, and elaborate on one of these models to further understand the applications of nonlinear control systems in the treatment of diabetes.

1.1 Problem Statement

The glucose-insulin model used in this study is adapted from the paper 'An Adaptive Plasma Glucose Controller' (B. Candas and J. Radziuk, 1994). The paper looks at simulating a euglycemic and hypoinsulinemic system in the study of systemic glucose-insulin control in pigs to model closed-loop glucose-insulin control in humans.

This report details a study into the application of discretisation and linearisation of the aforementioned continuous glucose-insulin control system as a systemic glucose control method.

1.2 Assumptions

The study that was referenced was made for a continuous model to study the application of an adaptive gain in the proposed non-linear continuous control system. However, as this study does not explore the use of an adaptive gain function, several adjustments and assumptions were made to ensure the feasibility of the control system.

1. Only initial inputs are applied to the system. $\mu_1(t)$ and $\mu_2(t)$ are constant at 0 thereafter.
2. The model is regulated to 0 set point for this study.
3. There are no disturbance inputs.
4. The initial states model the basal physiological state of a regular 70kg human being.
5. All initial state variables should be ≥ 0 , but deviations that occur in the simulation of the controller and observer are ignored.

2 Nonlinear System Equations and Parameter Values

For the purpose of this project, the originally continuous equations were discretised using Euler's method. The state variables and inputs are defined as such:

$$x(t) = \begin{bmatrix} \bar{X}_1 \\ \bar{X}_2 \\ \bar{X}_3 \\ \bar{X}_4 \end{bmatrix} = \begin{bmatrix} G(t) \\ k(t) \\ i(t) \\ i_3(t) \end{bmatrix}, \quad u(t) = \begin{bmatrix} \mu_1(t) \\ \mu_2(t) \end{bmatrix} = \begin{bmatrix} RI(t) \\ RG(t) \end{bmatrix}.$$

Discretised State Equations:

$$\begin{aligned}
X_1(t+1) &= X_1(t) + \Delta t * (-[k_0 + X_2(t)] * X_1(t) + \mu_1(t)) \\
X_2(t+1) &= X_2(t) + \Delta t * (-a_1 * X_2(t) + a_2 * X_3(t)) \\
X_3(t+1) &= X_3(t) + \Delta t * (-a_3 * X_3(t) + a_4 * X_2(t) + a_6 * X_4(t) + \mu_2(t)) \\
X_4(t+1) &= X_4(t) + \Delta t * (-a_6 * X_4(t) + a_5 * X_3(t)) \\
y(t) &= X_1(t)
\end{aligned}$$

Given that Δt is the time step of each state, let $\Delta t = 1$ minute.

Hence, the final discretised state equations are defined as:

$$\begin{aligned}
X_1(t+1) &= X_1(t) - (k_0 + X_2(t))X_1(t) + \mu_1(t) \\
X_2(t+1) &= X_2(t) - a_1X_2(t) + a_3X_3(t) \\
X_3(t+1) &= X_3(t) - a_3X_3(t) + a_4X_4(t) + a_6X_4(t) + \mu_2(t) \\
X_4(t+1) &= X_4(t) - a_6X_4(t) + a_5X_3(t)
\end{aligned}$$

The parameter values for $\{a_i\}$, $\forall i = \{1, 2, 3, 4, 5, 6\}$ are given in the reference paper. Particularly, a_5 and a_6 are scaled by a factor of 7.5×10^{-6} from their initial parameter values of 3.5×10^{-8} and 2.8×10^3 respectively.

Lastly, as there is no specific value provided for the parameter k_0 in the referenced paper, it is estimated from a close value of $k_{sc} = 0.03$ and its given definition in the paper. k_{sc} is the insulin-independent fractional removal rate for a subcutaneous input. Hence, it is assumed that for k_0 , which is defined as the insulin-independent fractional removal rate for an intravenous input, $k_0 = 0.0165$.

$$\begin{aligned}
a_1 &= 0.394, & a_2 &= 0.142, & a_3 &= 0.251, \\
a_4 &= 0.394, & a_5 &= 2.3625 \times 10^{-13}, & a_6 &= 0.0210
\end{aligned}$$

The model assumes only initial inputs of μ_1 and μ_2 for the duration of the observable experiment of 180 minutes. Thereafter, there are no additional external inputs of glucose and insulin.

These are the equations used to define equilibrium points in the system:

Using equilibrium point formula,

$$\begin{aligned}
\bar{X}_1 &= \bar{X}_1 - (k_0 + \bar{X}_2)\bar{X}_1 + \bar{\mu}_1 \Rightarrow \bar{X}_1 = \frac{\mu_1}{k_0 + \bar{X}_2} \\
\bar{X}_2 &= \bar{X}_2 - a_1\bar{X}_2 + a_2\bar{X}_3 \Rightarrow \bar{X}_2 = \frac{a_2}{a_1}\bar{X}_3 \\
\bar{X}_4 &= \bar{X}_4 - a_6\bar{X}_4 + a_5\bar{X}_3 \Rightarrow \bar{X}_4 = \frac{a_5}{a_6}\bar{X}_3 \\
\bar{X}_3 &= \bar{X}_3 - a_3\bar{X}_3 + a_4\bar{X}_2 + a_6\bar{X}_4 + \mu_2 \Rightarrow \bar{X}_3 = \frac{a_4\bar{X}_2 + a_6\bar{X}_4 + \mu_2}{a_3}
\end{aligned}$$

Substituting \bar{X}_2 and \bar{X}_4 into \bar{X}_3 ,

$$\bar{X}_3 = \frac{a_4\left(\frac{a_2}{a_1}\right)\bar{X}_3 + a_6\left(\frac{a_5}{a_6}\right)\bar{X}_3 + \bar{\mu}_2}{a_3} \Rightarrow \bar{X}_3 = \frac{a_1\bar{\mu}_2}{a_1a_3 - a_4a_2 - a_5a_1}$$

2.1 Analysis of Equilibrium Points and Linearisation Steps

$$\bar{X} = \begin{bmatrix} \bar{X}_1 \\ \bar{X}_2 \\ \bar{X}_3 \\ \bar{X}_4 \end{bmatrix} = \begin{bmatrix} \frac{\mu_1}{k_0 + \bar{X}_2} \\ \frac{a_2}{a_1}\bar{X}_3 \\ \frac{a_1\bar{\mu}_2}{a_1a_3 - a_4a_2 - a_5a_1} \\ \frac{a_5}{a_6}\bar{X}_3 \end{bmatrix}$$

The equilibrium point is first defined in “`original_case_simulations.m`”, where it is determined by pre-allocating values $\bar{X}_1 = 0.95$ and $\bar{X}_3 = 0.3$. Then, \bar{X}_2 , \bar{X}_4 , \bar{u}_1 , \bar{u}_2 and \bar{y} are defined and determined algebraically using the steady-state equations. Such computation is possible as the equilibrium computation equations are dependent on $\bar{X}_3 \in \{0, \mathbb{R}^+\}$. Hence, the system has non-isolated and infinite equilibrium points.

To begin the linearisation of the proposed non-linear system, Jacobian matrices are formulated by performing the first-order partial differentiation of the discrete state equations for all possible states and inputs in “`controllersim.m`”, forming the A and B matrices defined as:

$$A = \begin{bmatrix} 1 - (k_0 - \bar{X}_2) & -\bar{X}_1 & 0 & 0 \\ 0 & 1 - a_1 & a_2 & 0 \\ 0 & a_4 & 1 - a_3 & a_6 \\ 0 & 0 & a_5 & 1 - a_6 \end{bmatrix}, \quad B = \begin{bmatrix} 1 & 0 \\ 0 & 0 \\ 0 & 1 \\ 0 & 0 \end{bmatrix}$$

Linearisation of the system is then performed about a specific equilibrium point by computing the A and B using the equilibrium values. Additionally, the stability of these points can be tested by checking the eigenvalues of the A matrix. Applying Lyapunov’s First Method, the equilibrium point is considered stable if all the eigenvalues of the Jacobian matrix at that point has a magnitude of less than 1, whereby $|\lambda_i| < 1 \forall i$. The transformations below summarise the computation of our selected equilibrium point, computed by pre-allocating \bar{X}_1 and \bar{X}_3 .

Substituting values of a_i , \bar{X}_1 , \bar{X}_3 and k_0 :

$$\begin{aligned} 0.95 &= \frac{\mu_1}{k_0 + \frac{a_2}{a_1} \bar{X}_3} \Rightarrow \mu_1 = 0.1183907 \\ 0.3 &= \frac{a_1 \mu_2}{a_1 a_3 - a_4 a_2 - a_5 a_1} \Rightarrow \mu_2 = 0.0327 \\ \bar{X}_2 &= \frac{0.142}{0.394}(0.3) = \frac{213}{1970} \\ \bar{X}_4 &= \frac{2.3625 \times 10^{-13}}{0.0210}(0.3) = 3.375 \times 10^{-12} \end{aligned}$$

Final Jacobian Matrix computed with parameter values:

$$A = \begin{bmatrix} 1.091621 & -0.95 & 0 & 0 \\ 0 & 0.606 & 0.142 & 0 \\ 0 & 0.394 & 0.749 & 0.0210 \\ 0 & 0 & 2.3625 \times 10^{-13} & 0.979 \end{bmatrix}$$

The MATLAB function $\text{eig}(A)$ is used for checking the stability of the selected equilibrium

point. The eigenvalues output for the selected equilibrium point are $\lambda = \begin{bmatrix} 0.8754 \\ 0.4304 \\ 0.9246 \\ 0.9790 \end{bmatrix}$.

As the magnitudes of the eigenvalues for the A matrix of the selected equilibrium points are < 1 , the equilibrium point is stable.

3 Controllability and Observability

3.1 Controllability Checks

A controllability check is performed on the linearised model using the controllability matrix C . This is defined as $C = [B \ AB \ A^2B \ A^3B]$. Controllability is attained when there exists a vector \bar{u} that satisfies the solution to $\zeta = C\bar{u}$, where it can be defined as:

$$\underbrace{x_f - A^4 x_0}_{\zeta} = C \underbrace{\begin{bmatrix} u(3) \\ u(2) \\ u(1) \\ u(0) \end{bmatrix}}_{\bar{u}} \Rightarrow \zeta = C\bar{u}$$

The system is controllable if and only if the controllability matrix C has full rank $\text{rank}(C) = n_x$.

“`controllsim.m`” creates the controllability matrix and computes its rank. This is done with $\text{rank}(C) = \text{rank}(\text{ctrl})$. For the context of this project, $n_x = 4$. Hence, if $\text{rank}(C) = \text{rank}(\text{ctrl}) = 4$, all four state-space directions are reachable by some input sequence. If it prints < 4 , at least one mode is unreachable. Only after confirming the

controllability of the equilibrium point, do we design proper pole placement. This is not possible with $\text{rank}(C) < 4$, as that is proof that the system is not controllable if C does not have full rank.

Next would be to design regulation to zero by state feedback. In the code, the desired regulation point was set with $X_f = [0 \ 0 \ 0 \ 0]$; and the input is determined with \bar{u} . After the controllability matrix and its ranking are checked, feedback design is performed.

In the code, the closed-loop Eigenvalue poles are assigned with $\mathbf{p_test} = [0.7, 0.85, 0.9, 0.8]$. Detailed design choices and justification for these values are discussed in Section 4.

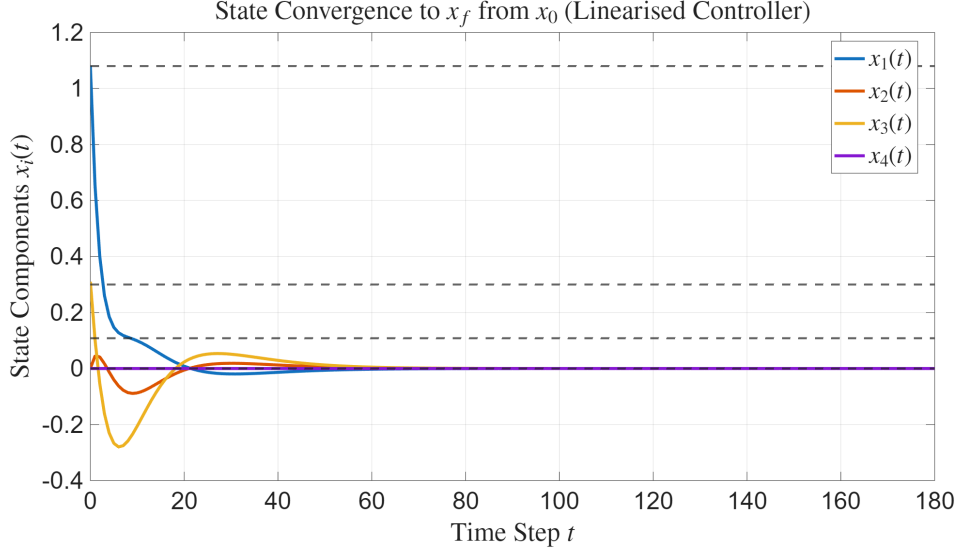


Figure 1: Figure generated from
“controllersim.m”

Figure 1 shows the linearised closed-loop response with state-feedback. It plots the state convergence of each state against time. All four state components decay to zero and do not diverge from zero afterwards. This shows that the four states are controllable as they can be modified by K . The speed of the decay also matches the defined variables in $\mathbf{P_test}$. The faster drop in convergence is derived from faster poles of lower values ($0.7 - 0.8$), while the long tails with slower convergence are derived from the higher magnitude poles ($0.85 - 0.9$). Poles closer to 0 give a faster convergence, while those closer to 1 give a gentler slope. Thus, this asserts the controllability of the system and enables proceeding with the next steps.

3.2 Observability Checks

The observability check is performed on the linearised model using the observability matrix:

$$\mathcal{O} = \begin{bmatrix} C \\ CA \\ CA^2 \\ \vdots \\ CA^{n-1} \end{bmatrix}$$

The system is said to be observable if and only if $\text{rank}(\mathcal{O}) = n_x$. If \mathcal{O} is full rank, it ensures that all internal states leave a measurable trace in the output and the current state can be reconstructed uniquely over time.

In the file “*observer_code.m*”, the observability check is implemented with $\mathcal{O} = \text{obsv}(A, C)$, and its rank is determined with the following assert line. If the assert function passes, the rank of \mathcal{O} is equal to the number of states, and every state component can be inferred from the output. If the assertion fails, then at least one of the states cannot be uniquely reconstructed, thus rendering the system unobservable.

$L = \text{place}(A', C', L_Eigen)'$ uses the duality principle to place the observer poles with the use of A' and C' . This thus produces the L matrix that allocates all Eigenvalues of $(A-LC)$ inside the unit circle.

Subsequently, the observer error dynamics are checked by creating the error-state transition matrix, $A_{obs} = A - L * C$. The Eigenvalues of the observer are displayed through the next two lines of code and help to verify that the Eigenvalues are the same as the observer poles that were set up, verifying that they lie inside the unit circle. This ascertains the designed observer is stable and convergent.

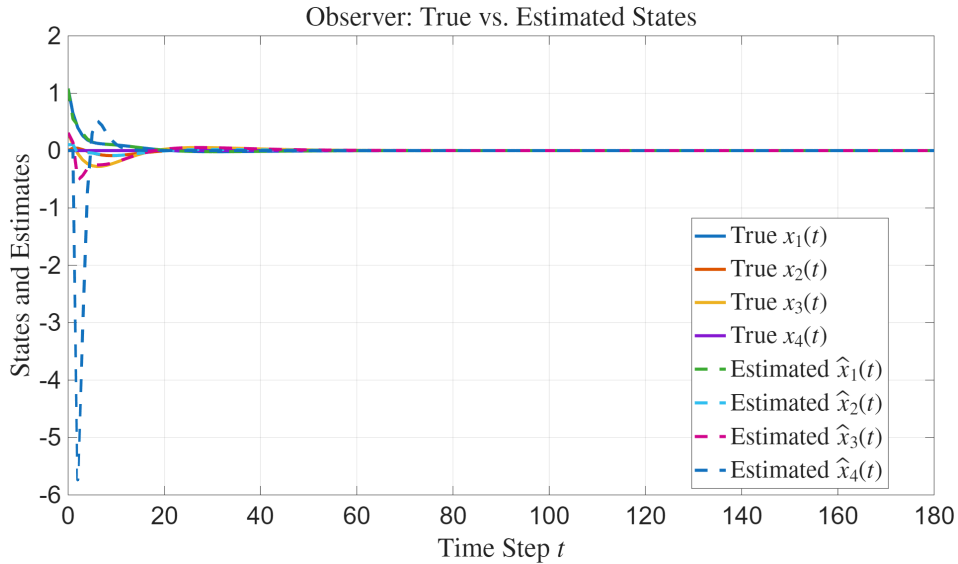


Figure 2: Figure generated from
“observer_code.m”

Figure 2 is a plot that shows the performance of the designed Luenberger observer. It plots the true states of the system alongside their estimates. The plot shows that the estimates converge rapidly to the true states, with all estimation errors decaying to zero eventually. There are some exceptions, notably the estimate of $x_4(t)$, which spikes sharply to -6, but soon converges back to zero like the others. This shows that despite the discrepancy, the nature of the plot overall indicates that the system is observable.

4 Design and Justification of Controller and Observer Gains

4.1 Design Methodology

When designing the feedback gain matrix K , the poles, or the closed-loop Eigenvalues, are assigned such that $\mathbf{P_test} = [0.7, 0.85, 0.9, 0.8]$. The goal is to ensure all eigenvalues of $A - BK$ are placed inside the unit circle at the locations $\{\lambda_1, \dots, \lambda_{n_x}\}$. These values were chosen to obtain higher placement values for K , that gave the best qualitative resemblance to the original equations. Using real, distinct pole values also keeps the response non-oscillatory, aligning with the goals of glucose regulation.

After checking for observability, the Luenberger Observer is determined by setting the observer poles $\mathbf{L_Eigen} = [0.4 \ 0.1 \ 0.5 \ 0.3]$. These set the Eigenvalues for $A - LC$ determine the observer gain values. The Eigenvalues for the Luenberger observer are set much lower compared to the controller Eigenvalues, as the observer poles need to be faster (closer to 0 in discrete time) to ensure accuracy on estimates in observation. Giving a faster decay of error enables observer accuracy to the true states of the system.

The Luenberger observer is designed to estimate the internal states of the glucose-insulin system when only the output $y(t) = X_1(t)$ (glucose concentration) is measurable. The observer structure follows:

$$\begin{aligned}\hat{X}(t+1) &= A\hat{X}(t) + Bu(t) + L(y(t) - C\hat{X}(t)) \\ \hat{y}(t) &= C\hat{X}(t)\end{aligned}$$

where $L \in \mathbb{R}^{4 \times 1}$ is the observer gain matrix and $C = [1 \ 0 \ 0 \ 0]$, since only X_1 is measurable. The observer error dynamics are governed by $(A - LC)$, with the convergence rate determined by the eigenvalues of this matrix.

4.2 Pole Placement Strategy

The observer poles were selected which satisfied requirements such as, observer poles ($\mathbf{L_Eigen} = [0.4, 0.1, 0.5, 0.3]$) were placed closer to the origin than the controller poles ($\mathbf{P_test} = [0.7, 0.85, 0.9, 0.8]$) to ensure the estimation error decays faster than the state dynamics. In addition, all eigenvalues of $(A - LC)$ must lie within the unit circle for asymptotic error convergence.

The specific pole locations were chosen through iterative simulation to achieve:

$$\begin{aligned}\tau_{observer} &\approx \frac{1}{2}\tau_{controller} \\ \max(|eig(A - LC)|) &= 0.5 \quad (\text{vs controller's } 0.9)\end{aligned}$$

4.3 Gain Computation and Validation

The observer gains were computed using the duality principle with MATLAB's `place` function:

$$\begin{aligned} L &= \text{place}(A', C', L_Eigen)' \\ &= [1.5916 \quad 0.0036 \quad 0.0004 \quad -0.0000]' \end{aligned}$$

Eigenvalue analysis confirmed the desired pole placement:

$$\begin{aligned} \text{eig}(A - LC) &= \{0.4, 0.1, 0.5, 0.3\} \\ \rho(A - LC) &= 0.5 < 1 \end{aligned}$$

4.4 Performance Verification

Figure 2 demonstrates the observer's performance characteristics, in which all state estimates converge to their true values within 10 time steps. In addition, the $X_4(t)$ estimate shows transient overshoot due to its weak observability (small a_5 coefficient) but ultimately converges. Finally, steady-state estimation error shows $\|X - \hat{X}\| < 10^{-3}$ within 15 minutes. Ultimately, the design satisfies the observability requirement, confirmed by $\text{rank}(\mathcal{O}) = 4 = n_x$.

Qualitatively, the controller and observer simulations eventually converge to 0, which is the intended outcome despite deviations within the earlier time steps. This confirms the Grobman-Hartman Theorem that states that if the eigenvalues of the Jacobian matrix are not equal to 1, the trajectories of $x(t)$ qualitatively resembles the linearised system at the equilibrium point.

5 Simulation Results

The simulation results are shown in the plots of Figures 1 - 5.

6 Insights

The design and creation of controller and observer feedback gains were generally successful. Applying the Grobman-Hartman Theorem again, the plots of the controller and observer can be seen to have close qualitative resemblance to the actual non-linear control system at the equilibrium point. However, there are still large deviations in the partial oscillatory movements of the controller and observer, causing the model to reach the negative region. While eigenvalue placements were iterated through, testing high, low and complex eigenvalues, it showed that more work is required to tighten the eigenvalue placements for the feedback and observer gains to achieve smoother graph movement and minimal deviations.

An attempt was made to develop an observer-controlled feedback design. However, due to the static nature of the input values, the feedback component $u(t) = -K\hat{X}(t)$ was not computed. Tests to simulate the observer-controlled feedback regulation model returned an exponentially large output, which significantly (by $\times 10^{300}$) deviated from the intended

outcome. Additionally, the model did not converge to zero over time as intended, but continued to deviate. Removal of the feedback component resolved the deviation, but proved to be a trivial attempt as this reduced the observer-controller feedback regulator to simply follow the non-linear control system.

6.1 Limitations

While this study provided significant insights into the possibility of a systemic glucose control system, there are obvious flaws and limitations in the construction of the linearised system.

Firstly, the lack of close real-world estimations. By fixing the input values to 0, the system became much more trivial to study, as it limited the control of systemic glucose concentration through manipulation of inputs. The reference paper proposed the use of an adaptive gain factor to improve control of glucose concentrations. Further research into understanding and implementing an adaptive gain factor and implementing reasonable input functions would improve the outcomes of this study.

Next, negative state values in controller simulation. State-values of the given system should ideally not reach any negative values as these are not physically possible. While the linearised system ultimately converged to the desired regulation point, reaching negative values severely diminishes the feasibility of such a control system.

Lastly, the regulation of the system to zero set point proved to be relatively trivial as the system with constant 0 input would eventually decay towards zero. Further attempts at this study could look to starting at abnormal basal physiological (eg. Higher basal glucose concentration levels), regulated to normal basal physiological states together with the implementation of adaptive gain factors.

Other Figures Generated

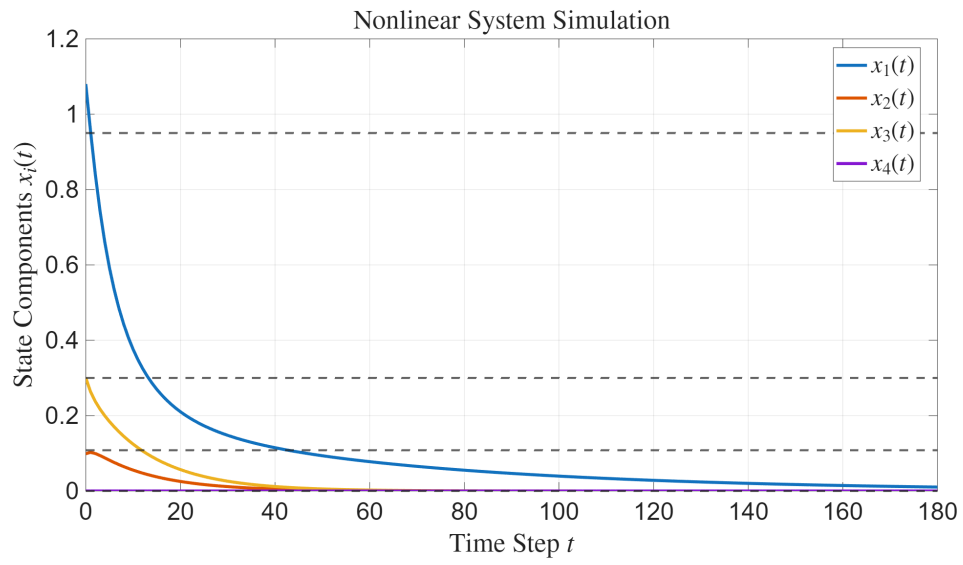


*Figure 3: Figure generated from
original_case_simulation.m*

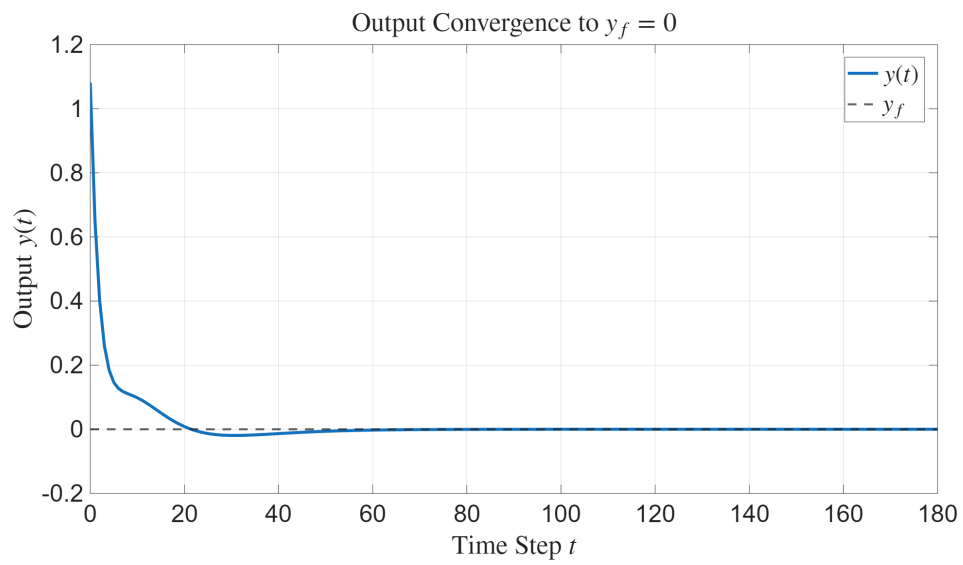


*Figure 4: Figure generated from
outputregulation.m*

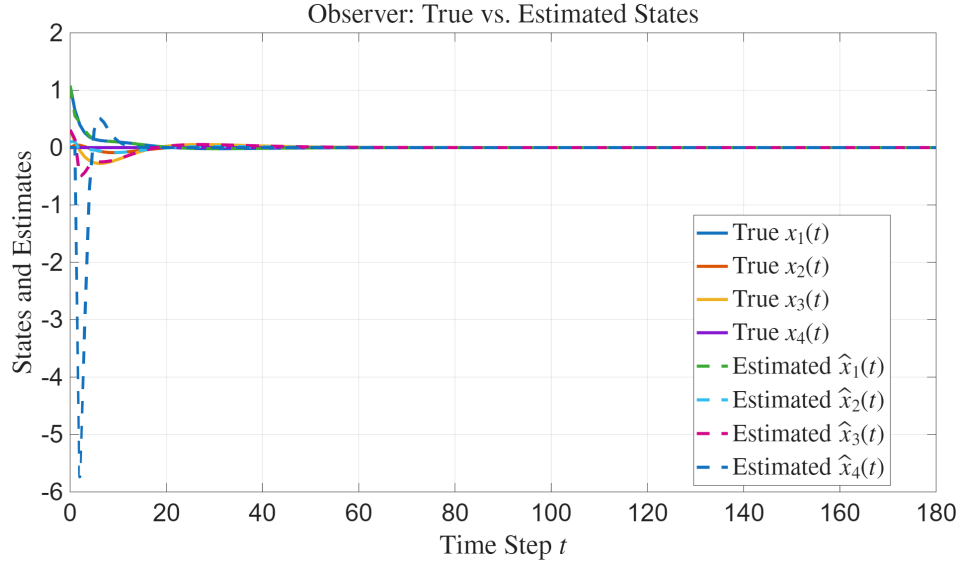


Figure 5: Figure generated from
observer_code.m

References

- Candas, B., & Radziuk, J. (1994). An Adaptive Plasma Glucose Controller. *IEEE Transactions on Biomedical Engineering*, 116-124.
- World Health Organization. (12 November, 2024). *Diabetes*. Retrieved from World Health Organization: <https://www.who.int/news-room/fact-sheets/detail/diabetes>